Journal of Pharmaceutical Chemistry
http://www.vensel.org/index.php/jphchem
VENSEL

De novo Design and *in-silico* Studies of Coumarin Derivatives as Inhibitors of Cyclin Dependent Kinase-2

[1]Ashok Sharma, [1]Badvel Pallavi, [1]Riddhidev Banerjee, [2]Mariasoosai Ramya Chandar Charles , [2]Mohane Selvaraj Coumar, [3]Subhash Chander, [3]Murugesan Sankaranarayanan, [1,*]Paritosh Shukla

[1]Department of Chemistry, Birla Institute of Technology and Science Pilani, Pilani campus, Pilani-333031, India
[2]Centre for Bioinformatics, School of Life Sciences, Pondicherry University, Kalapet, Puducherry-605014,India
[3]Department of Pharmacy, Birla Institute of Technology and Science Pilani, Pilani campus, Pilani-33031, India

Abstract: In the present study, around sixty-two novel coumarin derivatives were designed as CDK-2 inhibitors based on essential pharmacophoric requirements. All the designed compounds were subjected to docking study using AutoDock 4.2 against CDK-2 protein (PDB ID: 1HCK). Molinspiration and Osiris property explorer were used to predict Lipinski's rule of five and toxicity profile. The Structure Activity Relationship study revealed that, the substitution at R^1 and R^4 of coumarin nucleus enhances the binding energy and inhibitory constant values from nanomolar to picomolar range. Among the designed analogues, compound **15**, **28**, **43** and **59** showed significant binding energy and inhibitory constant values as compared to the standard drug Olomoucine and Deschloroflavopiridol. Most of the designed analogues showed similar binding mode and orientation inside the active site of the protein as that of the standard drug, which strongly indicates that the designed molecules may emerge as potent inhibitors of CDK-2. Next, molecular dynamics study of the significantly active molecule **15** was studied for 10 ns, in order to determine the stability of the coumarin molecules inside the binding cavity of the protein. *In-silico* investigations suggest that the *de novo* designed coumarin derivatives were potentially in-silico bioactive and need to be synthesized and tested further.

Keywords: Coumarine; CDK-2; anticancer; molecular docking; molecular dynamics

1. Introduction

For past three decades, computer-aided drug design methods[1] played a major role in the development of therapeutically significant small molecules and have also been helpful in toxicity prediction and optimization of several physiological properties including anticancer activity. These methods are broadly classified into structure-based or ligand-based methods. Structure-based methods are in principle analogous to high-throughput screening in both target and ligand and the structure information is overbearing. Structure-based approaches may include molecular docking, pharmacophore modeling, etc. Additionally, cancer cells are known to display deregulations in multiple signaling pathways, leading to uncontrolled cell proliferation and acquired anti-apoptosis properties.[2] Protein kinases are a large family of enzymes that are essential for the regulation of many diverse cell functions through phosphorylation of other enzymes and structural proteins.[3] In recent years, numerous biochemical and structural studies have contributed enormously to our increased understanding of the former's role in signal transduction[4] and cell cycle regulation[5]. This has led to better understanding of cancer mechanism. For example, crystal structures of several serine/threonine protein kinases, including cyclic-AMP dependent protein kinase (cAPK)[6], mitogen-activated protein kinase (MAPK)[7], casein kinase 1 (CK1)[8], phosphorylase kinase (PhK)[9] and cyclin-dependent kinase 2 (CDK2)[10] revealed, a common two-domain core structure with enzyme-specific variations[11]. Thus, cell cycle progression is regulated by a series of sequential events that include activation and subsequent inactivation of cyclin dependent kinases (CDK's) and cyclins and these CDKs form an active heterodimeric complex by binding to their regulatory subunits called "cyclins"[12]. Eleven members of the CDK family are reported so far out of which mainly CDK2, CDK4 and CDK6 work cooperatively to drive cells from G1 phase into S phase[13]. Furthermore, kinases can be blocked by small molecules and recently, Polo-like-kinases[14] and Aurora kinases[15] have been studied as potential targets for cancer therapy with fewer side effects than traditional cytotoxic drugs. Among protein kinases, CDK2 plays a central role in cell cycle regulation and efforts are under

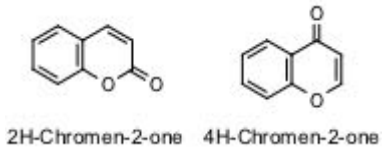

Figure 1. Structure of benzopyrones

Submitted on: May 26, 2017; Resubmitted on: Oct 4, 2017
Revised on: Oct 23, 2017
Accepted on: Oct 28, 2017
*corresponding author: PS - E-mail: shukla_p@pilani.bits-pilani.ac.in

-way to develop specific inhibitors of CDKs as potential antimitogenic drugs[16] The detailed structural analysis of CDK2 can provide valuable information for the design of new ligands that can bind in the ATP binding pocket and inhibits CDK2 activity[17]. Thus, we concentrated our efforts towards developing small-molecules that inhibit CDKs as most of the currently available agents targets the ATP-binding site of these enzymes[18]. Such an approach might create serious problems as catalytic residues are well conserved across eukaryotic protein kinases[19]. However, compounds such as Flavopiridol, Olomoucine and Butyrolactone-1 that exhibit greater specificity for CDKs have shown promising effect[20]. In the present study, main focus is to develop coumarin molecules as CDK-2 inhibitors because of various biological properties possessed by coumarin pharmacophore such as antitumor, anti-HIV, anticoagulant, anti-inflammatory and as CNS-active compounds. In addition, they also exhibit enzyme inhibition properties, antimicrobial and antioxidant activities also[21].

Coumarins are a group of compounds belonging to the benzopyran family isolated from plant product Tonka bean, *coumarou* in 1820 (Figure 1).[22] Benzopyrones are subdivided into benzo-α-pyrones and benzo-γ-pyrones of which coumarins and flavonoids are prime members of benzo-α-pyrones and benzo-γ-pyrones class respectively. Dietary exposure to benzopyrones is quite significant, as these compounds are found in vegetables, fruits, seeds, nuts, coffee, tea and wine. It is estimated that, the average western diet contains approximately 1g/day of mixed benzopyrones. It is therefore, quite logical to see why extensive research into their pharmacological and therapeutic properties is underway over many years. Researchers have also proved that the selective cytotoxicity of coumarins for tumor cells and also the effect of coumarins in the regulation of immune response, cell growth and differentiation.[23] The mechanism of action of anti-tumor drugs is basically to target the dividing cells that interrupt cell division. Although, new techniques like chemotherapy and radiotherapy can provide best results for the treatment of cancer but these trigger various side effects like nausea, hair loss, nervousness, skin soreness, etc. Coumarins are effective not only for the treatment of cancers like malignant melanoma, renal cell carcinoma, leukemia,[24] prostate cancer and breast cancer,[25] but also to treat the side effects caused by radiotherapy. The relapse of melanoma diagnosis has been minimized by the use of 4-hydroxy coumarin along with warfarin to maintain therapy and to inhibit the spreading of tumor cells.[26] In case of leukemia, prostate and breast cancer, cyclin D1 is released more than normal levels and coumarin derivatives have also been found very effective anti-proliferative agents by regulating the release of cyclin D1.[27]

Several researchers have reported various anticancer coumarin based drugs e.g. Genistein, Imperatorin, Osthole, Esculetin,[28] Fraxin, Grandivittin, Chartreusin and Demethylchartreusin[29] etc. It has been established that, some coumarin compounds including coumarin and 7-hydroxycoumarin, inhibit the cell growth of various types of cancer cell lines.[30] In one study, no adverse effects of coumarins were reported in humans using doses up to 7 g /day, even after two weeks of continued treatment.[31]

The biochemical, pharmacological and therapeutic applications of simple coumarins could be influenced by their substitution pattern. This, coupled with our interest in anticancer drug discovery[32] motivated us to design novel coumarin derivatives as CDK-2 inhibitors and to explore the effect of the substitution of OH group of the coumarin with various heterocyclic moieties at R1, R2, R3 and R4 positions i.e. 3-, 4-, 6-, and 7th positions respectively. The general structures of all the designed analogues are shown in Figure 2. Furthermore, the molecular dynamics (MD) study was also performed for the *in-silico* significantly active molecules in order to predict the time evolution of a target protein with designed ligands.

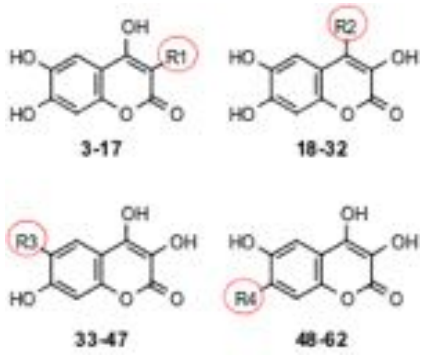

Figure 2. Designed analogues

2. Result and Discussion

2.1. Molecular docking simulation

Docking is an approach to rational drug design and very much helpful in predicting the structure and binding free energy of ligand-receptor complex. It gives us the information on how the ligand molecule bind with the receptor and what amino acid residues are involved in providing flexibility to it. The molecular modeling software AutoDock 4.2 has been used for the docking of all designed sixty-two coumarin molecules. The molecular dynamics study of the significantly active molecules inside the pocket of the protein was also subsequently performed. The docking was performed using THR14 (T) and TYR15 (Y) residues of the GTYG cluster of ATP binding sites (residues 13 to 16, PDB Code:1HCK) as flexible ones.

Validation of docking: Prior to docking of designed analogues, validation of docking protocol is very important. The validation of docking was done by extracting out the co-crystallized ATP of the target protein CDK-2 and then docked back into the active site of the receptor. It was evident that, the docked pose of the re-docked ATP was almost superimposed with that of the co-crystallized ligand with acceptable root mean square deviation of 0.85 Å (Figure 3). Subsequently, the Mg-ATP hydrogen-bonding (pink dotted line) and hydrophobic interaction (green dotted line) with the receptor protein was also determined for validation and are shown in Figure 4. The reproducibility and the reliability of the docking parameters has been done by docking of the standard drug (Olomoucine and Deschloroflavopiridol) with target protein. Hydrogen bonding and hydrophobic interaction of the standard drug with the active site amino acid residues of 1HCK protein is shown in Figure 5 (Deschloroflavopiridol) and Figure 6 (Olomoucine) respectively.

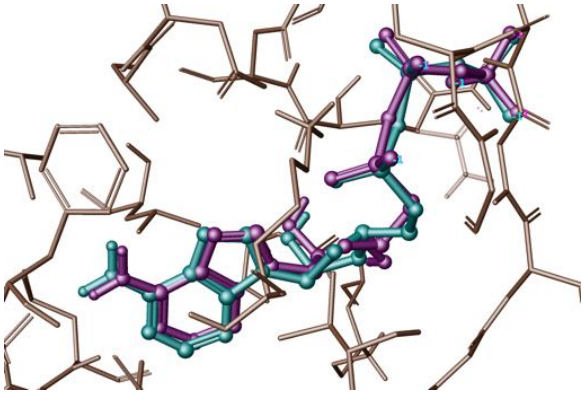

Figure 3. Validation by redocking, redocked ATP (in green ball & stick) superimposed on co-crystalliaed Mg-ATP (Violet ball & stick) in binding pocket of CDK-2 (PDB: 1HCK)

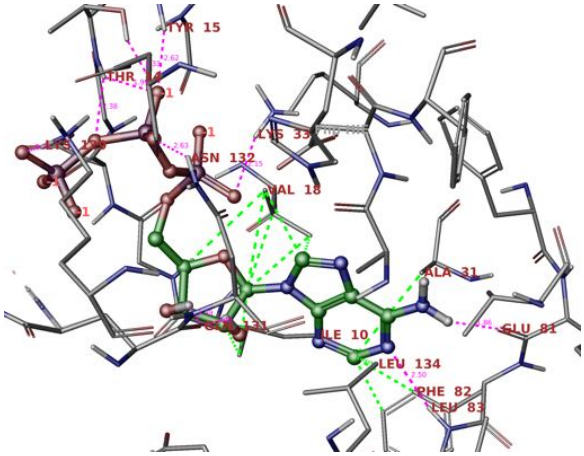

Figure 4. H-bonding (pink dotted line) and hydrophobic (green dotted line) interaction of co-crystallized ATP with CDK-2 (PDB: 1HCK)

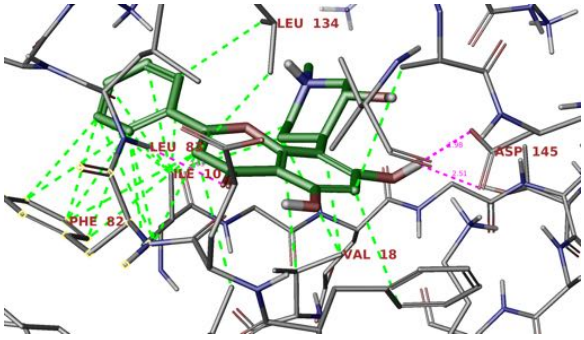

Figure 5. Deschlorflavopiridol (tube coloured by atom type) in ATP binding sit of 1HCK. H-bonding interaction in pink dotted line & hydrophobic interaction in green dotted lines.

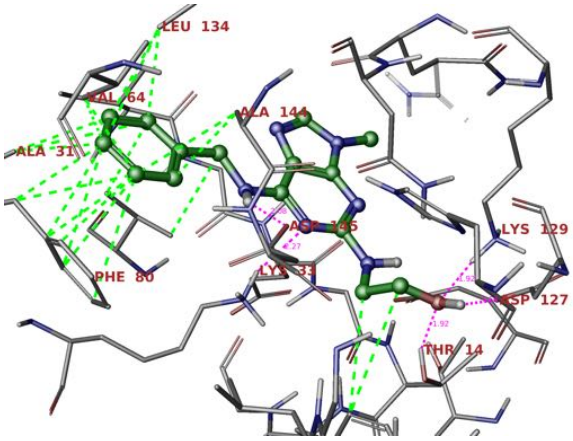

Figure 6. Olomoucine (ball& stick coloured by atom type)at ATP binding site of 1HCK. H-bonding interaction in pink dotted line & hydrophobic interaction in green dotted lines.

Docking Outcomes and Discussion: The docking parameters such as binding free energy (Kcal/mol) and predicted inhibitory constant (Ki) for all sixty-two designed analogs were determined and are shown in Table 1a-d. Compounds showing high binding energy (negative) have lower enzyme inhibitory constant value and vice versa. In the present study, the designed analogs showed binding free energy values in the range of -12.07 to -8.06 upon varying the substitution at position 3 (Table 1a); -11.87 to -8.02 when variation is made at position 4 (Table 1b); -12.72 to -10.06 when variation is performed at position 6 (Table 1c) and -12.50 to -8.35 when variation is done at position 7 (Table 1d) of the designed coumarin molecule with different heterocyclic moieties. Among the designed sixty-two analogs, compounds 14, 15, 41, 42, 43, 47, 53, 58 and 59 showed significant binding free energy values of -12.00, -12.07, -12.10, -12.68, -12.72, -12.13, -12.01, -12.38 and -12.50 kcal/mol respectively against CDK-2 receptor with that of standard Deschloroflavopiridol

Table 1a. Estimated docking scores for 1-17

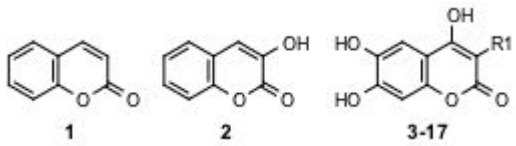

Code	R1	Estimated	
		[1]BE	[2]K_i
1	H	-9.21	177.54
2	OH	-9.36	138.01
3	3-(benzo[b]thiophen-2-yl)	-8.06	1230
4	3-(benzo[b]thiophen-3-yl	-11.74	2.49
5	3-(benzofuran-2-yl)	-11.90	1.90
6	3-(benzofuran-3-yl)	-10.15	36.11
7	3-(1H-isoindol-3-yl)	-11.04	8.05
8	3-(1H-indol-3-yl)	-10.51	19.94
9	3-(1H-indol-2-yl)	-10.29	28.81
10	3-(1H-indazol-3-yl)	-11.24	5.79
11	3-(1H-benzo[d]imidazol-2-yl)	-11.81	2.19
12	3-(quinolin-2-yl)	-10.42	23.07
13	3-(quinolin-3-yl)	-11.05	7.96
14	3-(quinolin-4-yl)	-12.00	1.59
15	3-(quinazolin-2-yl)	-12.07	1.41
16	3-(indolin-2-yl)	-10.86	11.04
17	3-(1,2,3,4-tetrahydroquinolin-2-yl)	-10.48	20.79

[1]BE-Binding Energy in kcl/mol; 2K_i-Inhibition constant in nM

Table 1b. Estimated docking scores for 18-32 (Fig 2)

Code	R2	Estimated	
		[1]BE	[2]K_i
18	4-(benzo[b]thiophen-2-yl)	-8.80	352.65
19	4-(benzo[b]thiophen-3-yl)	-8.02	1.33
20	4-(isobenzofuran-1-yl)	-9.44	121.30
21	4-(benzofuran-3-yl)	-8.54	549.10
22	4-(1H-isoindol-3-yl)	-10.05	43.06
23	4-(1H-indol-3-yl)	-10.71	14.19
24	4-(1H-indol-2-yl)	-10.81	11.94
25	4-(1H-indazol-3-yl)	-11.08	7.51
26	4-(1H-benzo[d]imidazol-2-yl)	-11.73	2.52
27	4-(quinolin-2-yl)	-10.97	9.04
28	4-(quinolin-3-yl)	-11.87	2.00
29	4-(quinolin-4-yl)	-10.05	43.16
30	4-(quinazolin-2-yl)	-10.49	20.34
31	4-(indolin-2-yl)	-8.97	264.61
32	4-(1,2,3,4-tetrahydroquinolin-2-yl)	-11.16	6.59

[1]BE-Binding Energy in kcl/mol; 2K_i-Inhibition constant in nM

Table 1c. Estimated docking scores for 33-47 (Fig 2)

Code	R3	Estimated	
		[1]BE	[2]K_i
33	6-(benzo[b]thiophen-2-yl)	-11.32	5.05
34	6-(benzo[b]thiophen-3-yl)	-10.39	24.22
35	6-(benzofuran-2-yl)	-10.83	11.53
36	6-(benzofuran-3-yl)	-11.09	7.37
37	6-(1H-isoindol-3-yl)	-10.06	42.23
38	6-(1H-indol-3-yl)	-11.13	6.92
39	6-(1H-indol-2-yl)	-11.91	1.87
40	6-(1H-indazol-3-yl)	-11.70	2.65
41	6-(1H-benzo[d]imidazol-2-yl)	-12.10	1.35
42	6-(quinolin-2-yl)	-12.68	0.51
43	6-(quinolin-3-yl)	-12.72	0.48
44	6-(quinolin-4-yl)	-10.71	14.22
45	6-(quinazolin-2-yl)	-11.96	1.71
46	6-(indolin-2-yl)	-11.45	4.08
47	6-(1,2,3,4-tetrahydroquinolin-2-yl)	-12.13	1.28

[1]BE-Binding Energy in kcl/mol; 2K_i-Inhibition constant in nM

Table 1d. Estimated docking scores for 48-62 (Fig 2)

Code	R4	Estimated	
		[1]BE	[2]K_i
48	7-(benzo[b]thiophen-2-yl)	-9.31	149.34
49	7-(benzo[b]thiophen-3-yl)	-10.34	26.29
50	7-(benzofuran-2-yl)	-10.88	10.63
51	7-(benzofuran-3-yl)	-8.35	759.88
52	7-(1H-isoindol-3-yl)-	-11.18	6.33
53	7-(1H-indol-3-yl)-	-12.01	1.57
54	7-(1H-indol-2-yl)	-9.85	60.71
55	7-(1H-indazol-3-yl)	-11.24	5.78
56	7-(1H-benzo[d]imidazol-2-yl)	-11.39	4.45
57	7-(quinolin-2-yl)	-10.42	23.07
58	7-(quinolin-3-yl)	-12.38	0.84
59	7-(quinolin-4-yl)	-12.50	0.69
60	7-(quinazolin-2-yl)	-11.50	3.73
61	7-(indolin-2-yl)	-11.28	5.38
62	7-(1,2,3,4-tetrahydroquinolin-2-yl)	-11.40	4.37

[1]BE-Binding Energy in kcl/mol; 2K_i-Inhibition constant in nM

(-8.87) and olomoucine (-6.08 kcal/mol). The binding free energy in decreasing order exhibits the following trend for the designed ligands: 43 > 42 > 59 > 58 > 47 > 41 > 15 > 53 > 14. From the binding free energy trend we infer that, compound 43 is the most significantly active CDK-2 inhibitor. Closer observation of receptor-ligand complex reveals that, the designed analogs adopt the same conformation in the ATP active site of CDK-2 as do other standard CDK-2 inhibitors. Hydrogen bonding and hydrophobic interactions were observed between ligands and amino acids of the receptor protein. These interactions play an important role in the determination of binding free energy and stability of receptor-ligand complex.

Structure-Activity-Relationship (SAR): A brief SAR (Figure 7) is quite unambiguous. Comparing the binding free energy values of the designed coumarin analogs, it was observed that, upon varying the substitution at 6th position i.e. R^3 fragment as compared to R^1, R^2, and R^4, the B.E (Kcal/mol) increases and most of the designed molecules like 41, 42, 43 and 47 showed excellent binding free energy and inhibitory constant values. Although, in some molecules, upon varying the substitution at 7th position i.e. R^4 of the coumarin molecule, significant binding free energy and inhibitory constant values are exhibited, e.g. compound 53, 58 and 59. But still closer observation reveals that, the substitution at 6th position of the coumarin analogs is the appropriate position where a desired substitution may lead to enhanced inhibitory activity of protein CDK-2. Thus, overall significant binding free energy and inhibitory constant values are in the order as $R^3 > R^4 > R^1 > R^2$ (i.e. position 6 > 7 > 3 > 4). Hence, some SAR inferences are unequivocal: (a) substitution by a heterocycle at the 6th position invariably leads to excellent binding (b) a similar substitution at the 7th position also leads to good binding ability. The reason behind this better activity of the 6th and 7th position substituted coumarin molecule may be because of the reduced steric hindrance caused by the substituted heterocyclic molecules at these positions. (c) Another interesting observation was, when quinolinyl, quinazolinyl, indazolyl and indolyl type moieties are present as substituents, better score was obtained irrespective of the substitution position (i.e. whether the substitution occurs at R^1, R^2, R^3 or R^4) of the coumarin molecule. But still the substitution at 6th position remains the best with respect to all other positions. The substitution of the benzothiophenyl fragment in coumarin molecule shows lower binding free energy at all the positions of the coumarin molecule and is one of the exceptional case predicted during observation of Table 1a-d. Finally, molecular dynamics simulation study was performed in order to find out the stability of the significantly active compound from each studied position of the coumarin molecule inside the binding pocket of the target protein molecule.

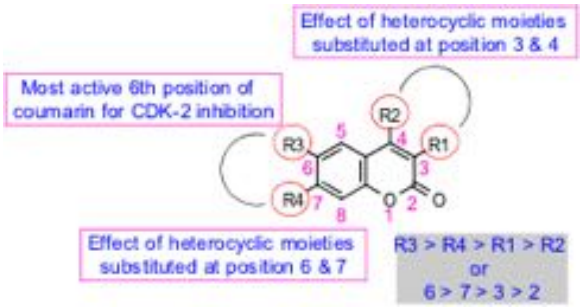

Figure 7. SAR of designed analogues

Hydrogen Bonding Interaction: In Figure 8a, the 2D interaction pattern of compound 15 (3-17) shows that, all the atoms responsible for H-bonding behave as H-bond acceptors. Here, the -OH group present at 3rd position was substituted by quinolin-2-yl. The hydrophilic oxygen of the -OH group at 4th position of coumarin forms hydrogen bond with the adjacent

LYS33 amino acid. The 6th and 7th position of coumarin in compound 15 showed hydrogen bonding interaction with THR14 and LYS129 respectively whereas hydroxyl group at 6th and 7th position behaves as H-bond acceptor and the corresponding amino acids as H-bond donors. LYS129 showed H-bonding with both the substituted hydroxyl group at 6th and 7th position of the coumarin molecule. The corresponding 3D interaction pattern of the designed ligand 15 with the receptor amino acids are shown in Figure 8b.

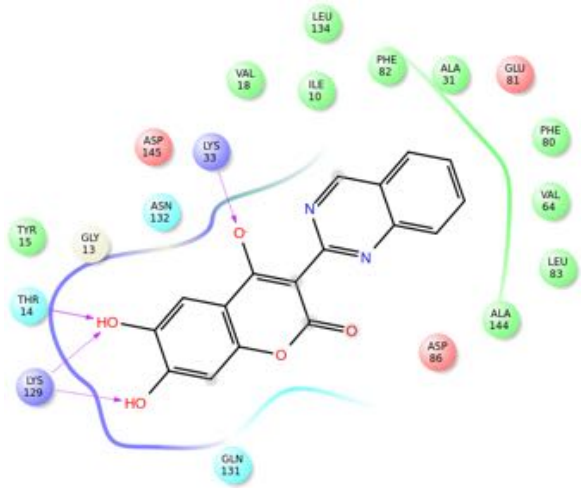

Figure 8a. 2-Plot of compound 15

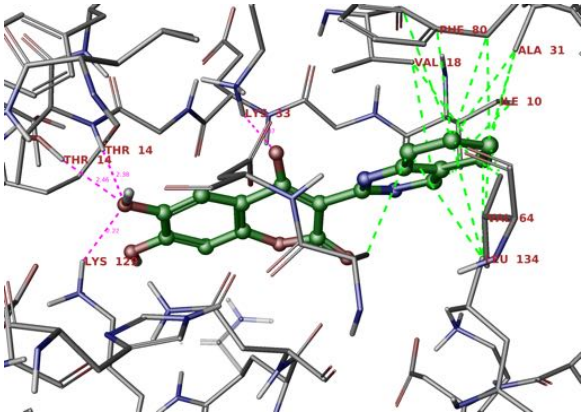

Figure 8b. 3D-plot of compound 15

Similarly, Figure 9a and Figure 9b showed the interaction mode of the molecule 28 (18-32) with various amino acids in 2D and 3D views respectively. Here, the hydroxyl group at 4th position of the designed ligand was substituted by quinolin-3-yl moiety. A close observation of 2D view of Figure 9b showed that, almost all the heteroatoms of the designed ligand behave as H-bond donors. Here, the H (Hydrogen) of the substituted -OH group at 3rd position of coumarin forms H-bond with ASP145. The H of the -OH group substituted at 6th and 7th position of coumarin showed H-bonding with LEU83. Also, LEU83 appears to form bifurcated H-bond with both the H atom of the -OH group present at 6th and 7th position of coumarin molecule.

Figure 10a and Figure 10b showed the 2D and 3D view of the various interactions of the designed ligand 43 (33-47,) with target protein. All the heteroatoms responsible for H-bonding behave as H-bond acceptors. The 6th position of the designed ligand 43 was substituted with quinolin-3-yl group. Oxygen of the keto group which behaves as H-bond acceptor forms H-bond with LYS129. The Hydroxyl group at the 3rd position of the designed ligand forms bifurcated H-bond i.e. one with LYS129 and the other with THR14. The Oxygen atom of the -OH group at the 4th position of the designed ligand forms H-bond with LYS33.

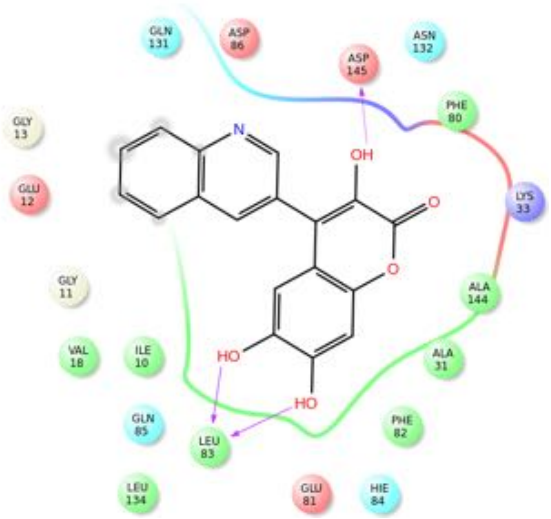

Figure 9a. 2D-plot of compound 28

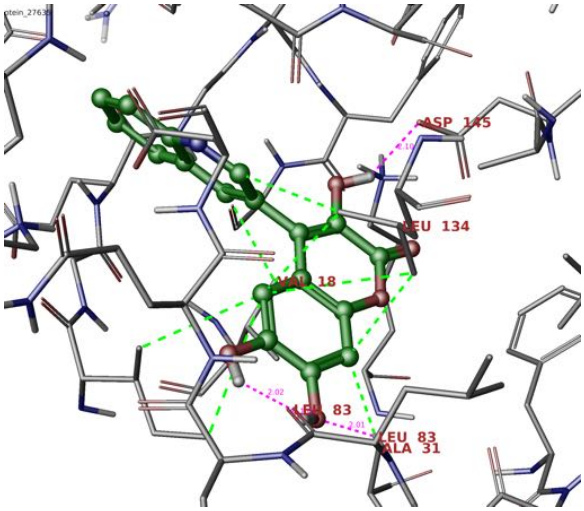

Figure 9b. 3D-plot of compound 28

Similarly, Figure 11a and Figure 11b showed the 2D and 3D interaction style of the designed ligand 59 (48-62) where the -OH group at 7th position was substituted by quinolin-4-yl moiety as shown in Table 1. Here, all the H-bond forming atoms of the ligand behave as H-bond donors. The -OH group present at 3rd and 6th position of the designed ligand forms H-bond with GLU12 and ASP86 respectively. The corresponding 3D view with bond distance is shown in Figure 11b. Overall, it was concluded that, the hydroxyl groups present in the designed ligands are responsible for H-bonding interaction inside the active site of the protein CDK2.

Hydrophobic Interaction: Although, the hydrophobic interactions are weak interactions unlike H-bonding interactions but play very important role in the stability of ligand-protein complex. According to Davis,[36] most of the marketed drugs consist of around 16 types of

hydrophobic atoms, with three to four acceptors and two to three donor atoms. These hydrophobic interactions not only play very important role in drug designing but are also very cooperative in increasing the binding affinity among the target drug and receptor protein.

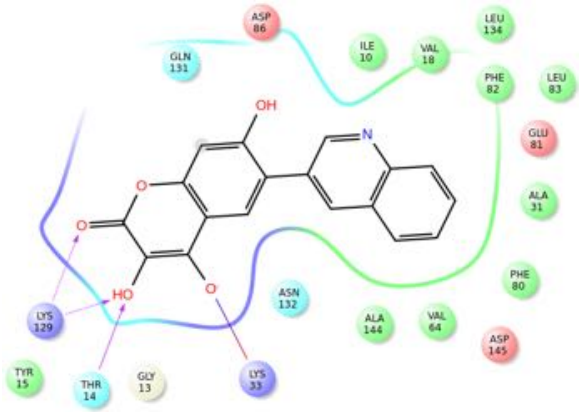

Figure 10a. 2D-plot of compound 43

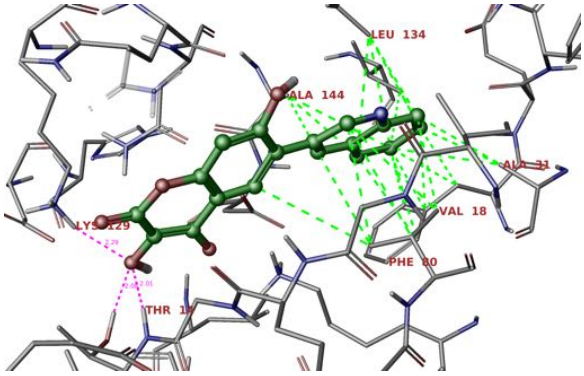

Figure 10c. 3D-plot of compound 43

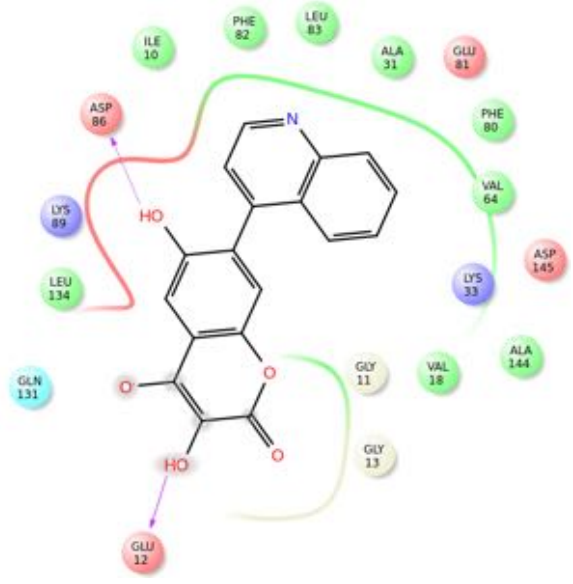

Figure 11a. 2D-plot for compound 59

The binding affinity of the drug molecule with target receptor can be increased by engineering the target or the drug or the interface between the drug and target receptor. The probability of the biological activity of the drug lead increases by increasing the number of hydrophobic atoms in the active core of drug-target interface.

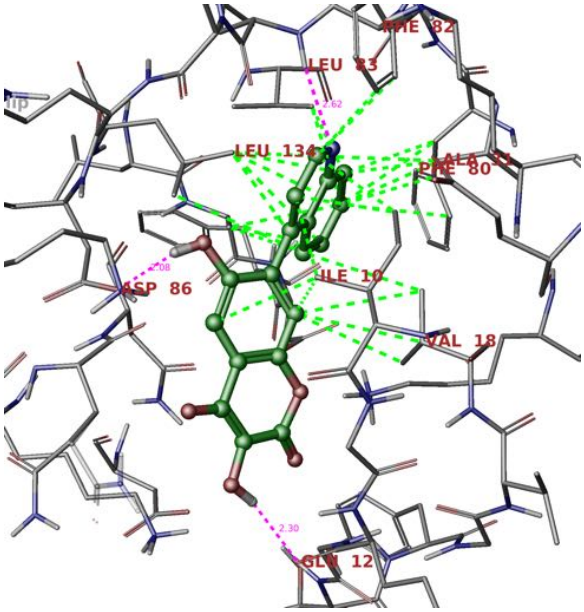

Figure 11b. 3D-plot for compound 59

All the green circled amino acids like VAL-18, ILE-10, LEU-134, PHE-82, ALA-31, PHE-80, VAL-64, LEU-83, ALA-144 and TYR-15 showed hydrophobic interaction with compound 15 (Figure 8a); PHE-80, ALA-144, ALA-31, PHE-82, LEU-83, LEU-134, ILE-10 and VAL-18 showed hydrophobic interaction with compound 28 (Figure 9a); ILE-10, VAL-18, LEU-134, PHE-82, LEU-83, ALA-31, PHE-80, VAL-64, ALA-144 and TYR-15 showed hydrophobic interaction with compound 43 (Figure 10a) while ILE-10, PHE-82, LEU-83, ALA-31, PHE-80, VAL-64, VAL-18, ALA-144 and LEU-134 showed hydrophobic interaction with compound 59 (Figure 11a). The corresponding 3D images with hydrophobic interactions of designed ligand 15, 28, 43 and 59 are shown in Figure 8b-11b respectively. All the hydrophobic interactions are shown by green dotted lines in Figure 8b-11b.

Electrostatic Interaction: In Figure 8a, the most common amino acids which showed electrostatic interaction with the designed ligand 15 are ASP-145, ASN-132, THR-14, GLN-131, GLU-81 and ASP-86. Designed ligand 28 showed electrostatic interaction with GLU-12, ASP-86, ASP-145, GLU-81, GLN-131, GLU-12, ASN-132 and GLN-85 amino acids as shown in Figure 9a. The amino acids responsible for ionic electrostatic interaction with the designed ligand 43 are THR-14, GLN-131, ASN-132, ASP-86, GLU-81 and ASP-145 as shown in Figure 10a. The designed ligand 59 showed electrostatic interaction with ASP-86, GLU-81, ASP-145, GLU-12 and GLN-131 amino acids as shown in Figure 11a.

All amino acids that showed electrostatic interactions are circled in red and dark blue color. The corresponding electrostatic interaction of all the designed ligand 15, 28, 43 and 59 in 3D view with green dotted lines are shown in Figure 8a-11a respectively.

2.2. Molecular Dynamics Simulations

Top scored THC analog along (compound 15) with CDK2 was simulated for 10 ns with GROMACS 5.0.4 to study the behavior of compound 15-CDK2 complex. Initial energy of the complex was -8.35×10^5 kJ/mol which was stable throughout the simulation with minor variations of $\pm$ 3.33×10^3 kJ/mol. Energy plot of the complex shows that, the overall energy minima is well

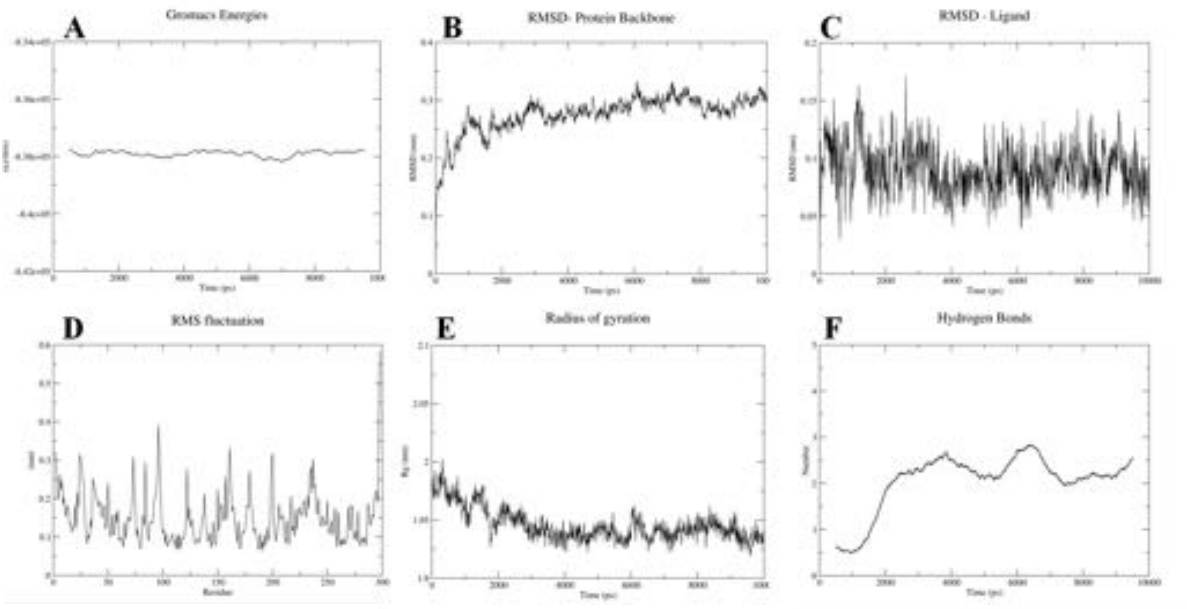

Figure 10. Molecular dynamic simulation of compound 15-CKD2 complex for 10 ns. (A) Potential energy of the complex, (B) RMSD of the protein backbone, (C) RMSD of the ligand, (D) RMSF of the amino acid residues, (E) Radius of gyration of complex and (F) Average number of H-bonds of the complex

maintained in the course of the simulation period (Figure 10a). Root mean square deviation shows that, the maximum deviation (Figure 10b) of the protein is 3.32Å in respect to the initial protein backbone, which means that all the ensembles of the protein-ligand complex conformations were within a deviation of 3.32 Å. Average RMSD value for the last 2 ns is 2.75 Å and at the end of the simulation was 3.06 Å. Throughout the simulation, average, maximum and minimum root mean square deviations of the ligand A-15 was 0.9, 1.71 and 0.29 Å, respectively (Figure 10c). Generally, validation of docking was done by re-docking the ligand present in the crystal structure. The deviation cutoff for the docked ligand to its original crystallized orientation is maximum 2 Å. In this aspect, lower RMSD value shows the stable interaction of the ligand inside the binding site of the CDK2.

Next, atomic fluctuations of the amino acid residues were calculated with respect to the initial equilibrated structure with Root Mean Square Fluctuation (RMSF) graph (Figure 10d). RMSF will helps find the local changes in the structure during the molecular dynamicssimulation. Typically, amino acids present in the C and N-terminal regions of the protein are more flexible than others. Alpha helix and beta strands are more rigid than the unstructured part of the protein. Sharp peaks in the RMSF plot indicate that, the residues are fluctuating more during simulation. A total of 294 amino acids were there in the protein; 58% of the amino acids (173 amino acids) were fluctuating between 1-2Å and 3.4% (10 amino acids) of the residues are fluctuating between 3-4 Å and are present in the loop portions of the CDK2. Lys298 and Arg297 residues are showing maximum fluctuations of 4-5 Å, which are present in the C-terminal of the protein.

Radius of gyration (Rg) value is a measure of the compactness of a protein which was calculated as RMS distance between the center of gravity and end of the protein. In other words, Rg is a measure assessing the stability of the folded protein. Radius of gyration of the initial starting structure was 1.97399 nm and the value decreased to 1.93452 nm at the end of 10 ns and MD simulation showed that compound 15-CDK2 complex was stable and well folded (Figure 10e). During the MD simulation, an average of 2-3 H-bonds were observed between compound 15 and CDK2 (Figure 10f) complex. Overall, MD simulation suggests that, compound 15 forms stable interaction with the target CDK2 protein.

2.3 Molecular parameters

Predicted molecular properties of the designed analogs are reported in Table 2. All the titled molecules were designed by heterocyclic molecular substitution at 3rd, 4th, 6th and 7th position of the tetrahydroxy coumarin (2) nucleus shown by 2 in Table 1. All the designed coumarin analogs follow Lipinski's rule of five. No violation of the Lipinski's rule was observed from Table 2. Some of the designed analogs like 18, 19, 20, 21, 22, 23, 24, 25, 26, 27, 28, 29, 30, 31, 32, 33, 34, 35, 36, 38, 39, 49, 51 and 53 showed high risk (++) on reproductive effect. Only two molecules 54 and 56 showed predicted high risk (++) and active risk (+) of producing mutagenicity respectively. Compound 14 showed active risk (+) of tumorigenicity. The high risk (++) of mutagenicity, tumorigenicity and reproductive effect is also shown by compound 1. However, risk alerts for the designed analogs may not be fully consistent and in order to evade risk of taking hazardous compounds, we screened off compound 1, 14, 18, 19, 20, 21, 22, 23, 24, 25, 26, 27, 28, 29, 30, 31, 32, 33, 34, 35, 36, 38, 39, 49, 51, 53, 54 and 56 molecules for further study. It should be noted that, these results are merely preliminary drug ability predictions and the calculations of toxicity are not analyzed in detail. In general, modification at 4th position of coumarins (Table 2) appears to increase high risk (++) on reproductive effect predicted in these molecules. The substitution at position 3 showed no side effect except compound 14, which showed the active risk of tumorigenicity (Table 2). The substitution

Table 2. Predicted molecular parameters of the designed analogs 1-62

Code	M. Wt (500)	C log P (5)	HBA (10)	HBD (5)	Solub.	Drug likeness	MUT	TUMO	IRRI	REP	Drug score
1	146.14	1.5	2	0	-2.37	-1.83	++	++	-	++	0.12
2	210.14	-0.08	6	4	-1.24	-1.87	-	-	-	-	0.55
3	326.32	2.6	5	3	-3.62	0.76	-	-	-	-	0.69
4	326.32	2.52	5	3	-3.51	-0.15	-	-	-	-	0.6
5	310.26	2.18	6	3	-3.45	0.21	-	-	-	-	0.66
6	310.26	2.13	6	3	-3.43	-0.28	-	-	-	-	0.61
7	309.27	1.2	6	3	-3.04	0.22	-	-	-	-	0.69
8	309.27	1.72	6	4	-2.79	0.72	-	-	-	-	0.74
9	309.27	1.77	6	4	-2.82	1.1	-	-	-	-	0.78
10	310.26	0.94	7	4	-2.37	1.56	-	-	-	-	0.83
11	310.26	1.17	7	4	-1.76	0.4	-	-	-	-	0.74
12	321.28	2.05	6	3	-3.0	-1.07	-	-	-	-	0.55
13	321.28	2.0	6	3	-2.97	-1.07	-	-	-	-	0.55
14	321.28	2.0	6	3	-2.97	-1.07	-	+	-	-	0.44
15	322.27	1.32	7	3	-2.05	-1.07	-	-	-	-	0.57
16	311.29	1.84	6	4	-2.96	2.35	-	-	-	-	0.83
17	325.32	2.19	6	4	-3.23	1.36	-	-	-	-	0.76
18	326.32	2.73	5	3	-4.26	0.59	-	-	-	++	0.37
19	326.32	2.64	5	3	-4.15	-0.33	-	-	-	++	0.33
20	310.26	2.31	6	3	-4.1	0.05	-	-	-	++	0.36
21	310.26	2.26	6	3	-4.07	-0.43	-	-	-	++	0.33
22	309.27	0.72	6	3	-3.05	0.05	-	-	-	++	0.4
23	309.27	1.84	6	4	-3.44	0.54	-	-	-	++	0.42
24	309.27	1.9	6	4	-3.46	0.92	-	-	-	++	0.44
25	310.26	1.07	7	4	-3.01	1.37	-	-	-	++	0.48
26	310.26	1.29	7	4	-2.41	0.22	-	-	-	++	0.42
27	321.28	2.17	6	3	-3.64	-1.26	-	-	-	++	0.3
28	321.28	2.12	6	3	-3.62	-1.26	-	-	-	++	0.3
29	321.28	2.12	6	3	-3.62	-1.26	-	-	-	++	0.3
30	322.27	1.45	7	3	-2.7	-1.26	-	-	-	++	0.33
31	311.29	1.37	6	4	-2.97	2.03	-	-	-	++	0.5
32	325.32	1.71	6	4	-3.24	1.05	-	-	-	++	0.45
33	326.32	3.01	5	3	-4.88	0.26	-	-	-	++	0.32
34	326.32	2.77	5	3	-4.86	-0.74	-	-	-	++	0.27
35	310.26	2.47	6	3	-4.48	-0.28	-	-	-	++	0.32
36	310.26	2.38	6	3	-4.78	-0.84	-	-	-	++	0.28
37	309.27	1.27	6	3	-3.93	-0.34	-	-	-	-	0.58
38	309.27	1.97	6	4	-4.15	0.15	-	-	-	++	0.37
39	309.27	2.06	6	4	-3.84	0.59	-	-	-	++	0.4
40	310.26	1.23	7	4	-3.09	0.98	-	-	-	-	0.75
41	310.26	1.51	7	4	-3.89	-0.12	-	-	-	-	0.6
42	321.28	2.34	6	3	-4.02	-1.64	-	-	-	-	0.46
43	321.28	2.24	6	3	-4.33	-1.64	-	-	-	-	0.44
44	321.28	2.24	6	3	-4.33	-1.64	-	-	-	-	0.44
45	322.27	1.67	7	3	-4.18	-1.64	-	-	-	-	0.46
46	311.29	1.85	6	4	-3.46	1.53	-	-	-	-	0.77
47	325.32	2.2	6	4	-3.72	0.56	-	-	-	-	0.66
48	326.32	3.01	5	3	-4.88	0.26	-	-	-	-	0.53
49	326.32	2.77	5	3	-4.86	-0.74	-	-	-	++	0.27
50	310.26	2.47	6	3	-4.47	-0.28	-	-	-	-	0.53
51	310.26	2.38	6	3	-4.78	-0.84	-	-	-	++	0.28
52	309.27	1.27	6	3	-3.93	-0.34	-	-	-	-	0.58
53	309.27	1.97	6	4	-4.15	0.15	-	-	-	++	0.37
54	309.27	2.06	6	4	-3.84	0.59	++	-	-	-	0.4
55	310.26	1.23	7	4	-3.09	0.98	-	-	-	-	0.75
56	310.26	1.51	7	4	-3.89	-0.12	+	-	-	-	0.48
57	321.28	2.34	6	3	-4.02	-1.64	-	-	-	-	0.46
58	321.28	2.24	6	3	-4.33	-1.64	-	-	-	-	0.44
59	321.28	2.24	6	3	-4.33	-1.64	-	-	-	-	0.44
60	322.27	1.67	7	3	-4.18	-1.64	-	-	-	-	0.46
61	311.29	1.85	6	4	-3.46	1.53	-	-	-	-	0.77
62	325.32	2.2	6	4	-3.72	0.56	-	-	-	-	0.66

HBA hydrogen bond acceptor, *HBD* hydrogen bond donor, *MUT* mutagenic, *TUMO* tumorigenic, *IRRI* irritant, *REP* reproductive effective, "+" active risk, "++" High risk "–" non-active risk

at 6th position showed high binding affinity with CDK-2 protein but some molecules showed high risk on reproductive effect also e.g. compounds 33, 34, 35, 36, 37, 39 and 40 (Table 2). Similarly, substitution at position 7 also showed no side effect except for very few molecules such as 49, 51, 53 and 56. The trend of decrease in side effect was observed from Table 2 and follows $R^2 > R^3 > R^4 > R^1$ (3 > 4 > 7 > 6). The detailed comprehensive study of the designed molecules are currently underway in our labs.

3. Conclusion

Thus, the physiological, anti-tumor and bacteriostatic activity marks coumarins as novel pharmacophores for

therapeutic applications. In the present study, around 62 novel coumarin analogs as CDK-2 inhibitors were designed based on pharmacophoric requirements. Docking study of the designed analogs was performed using molecular modeling software AutoDock 4.2. Among the designed analogs, compound 43 turns out into far better analogue overall. OSIRIS property explorer and molinspiration cheminformatics onlinetools were used to predict Lipinski rule of five parameter and toxicity parameters of the designed analogs. Among the designed analogs, compounds 4, 5, 11, 14, 15 (all 3-substituted), 25, 26, 27, 28, 32 (all 4-substituted), 41, 42, 43, 45, 47 (all 6-substituted), 53, 58, 59, 60 and 62 (all 7-substituted) showed significant binding free energy and predicted inhibitory constant values as compared to standard drug Deschloro flavopiridol and Olomoucine. Even though, compounds like 1, 14, 18, 19, 20, 21, 22, 23, 24, 25, 26, 27, 28, 29, 30, 31, 32, 33, 34, 35, 36, 38, 39, 49, 51, 53, 54 and 56 showed significant binding free energy and predicted inhibitory constant values, they have been screened off for next level of study because of their predicted poor pharmacokinetic and toxicity profile. From this study, it was concluded that, hydrogen bond donor and hydrogen bond acceptor groups in pharmacophore are very much important to form stable receptor-ligand complex as well as for better inhibitory potency. The molecular dynamics and simulation study was also performed for selected significantly active analogs to find out the stability of the molecules inside the binding pocket of the CDK-2 protein.

4. Experimental

Materials and methods: Molecular modeling software AutoDock 4.2 downloaded from www.scripps.edu was used for the entire docking study and the molecular dynamic simulation study was performed using GROMACS 5.0.4 molecular dynamics package software for 10 ns. CDK-2 enzyme (PDB ID: 1HCK) co-crystallized with Mg-ATP ligand was used as target receptor. Standard drug Olomoucine and Deschloroflavopiridol were used for calibration and validation of the docking protocol.

4.1. Molecular Docking protocol

The target protein, Cyclin Dependent Kinase-2 enzyme (PDB ID: 1HCK) was downloaded from RCSB protein data bank. Target protein preparation was done by removal of water molecules, by adding polar hydrogens and kollmann charges. A grid spacing of 0.375 Å and 60 ×60× 60 number of points was used for the docking study of all the designed molecules. The grid was centered on the active site. The auto grid program generated separate grid maps for all atom types of the ligand structures and one for electrostatic interactions. The PRODRG online server (http://davapc1.bioch.dundee.ac.uk/prodrg/) was used to minimize the conformational energy of the designed ligands in pdb format.[34] The Gasteiger-Huckel charges have been calculated for the energy minimized confirmations and saved in the default format of the AutoDock. AutoDock generated 50 possible binding conformations i.e., 50 runs for each docking using LGA search. Default protocol was applied with initial population of 150 randomly placed individuals, amaximum number of 2.5×10^5 energy evaluations and 2.7×10^4 generations. A mutation rate of 0.02 and a crossover rate of 0.8 were used.[35]

4.2. Molecular dynamics protocol

Ligand-target complex was simulated with GROMACS 5.0.4 molecular dynamics package to assess the stability. Gromos43a2 force field was used do define the atom types. Ligand parameters were obtained from PRODRG (http://davapc1.bioch.dundee.ac.uk/cgi-bin/prodrg) server. Ligand-CDK2complex was placed in a cubic box filled with SPC water molecules and the system was neutralized by the addition of required number of Na^+ and Cl^- ions. Then the system was minimized with steepest descent algorithm. Energy minimized system was equilibrated at 300 K for 150 ps followed by equilibration at 1 atm pressure for 150 ps. Production dynamics was carried out for 10 ns and the trajectories were analyzed with the available programs within the GROMACS package with default parameters.

4.3. Molecular parameters

Toxicity profile and good pharmacokinetic properties are very much decisive for any ligand to complete drug discovery process and to become a successful drug candidate. Hence, in the present work, Lipinski's rule of five parameters and toxicity properties of the designed coumarin ligands were predicted by molinspiration cheminformatics (http://www.molinspiration.com/) and OSIRIS property explorer (http://www.organic-chemistry.org/prog/peo/) respectively. The activity and selectivity increases by stepwise optimization of the pharmacological lead structure and their drug like physicochemical properties during drug discovery are confirmed by Lipinski's rule of five.[33]

In-silico prediction of compound toxicity / toxicity risk is important. Hence, in the present work, toxicity risks like mutagenicity, tumorigenicity, irritancy and the effect on sexual reproduction has also been predicted for all the designed analogs as shown in the Table 2.

Acknowledgement

P.S. would like to thank the University Grants Commission (UGC), New Delhi, India, for grant vide F. No 41-289/2012(SR). The authors would like to thank BITS-Pilani for providing the facilities to do this work. A.S. acknowledges BITS-Pilani for financial support in the form of Institute Research Fellowship.

References

1. Sliwoski, G.; Kothiwale, S.; Meiler, J.; Lowe, E. W. Computational Methods in Drug Discovery. Pharmacol Rev 2013, 66 (1), 334.
2. Meier, P.; Finch, A.; Evan, G. Apoptosis in development. Nature 2000, 407 (6805), 796-801.
3. Hanks, S. K.; Quinn, A. M.; Hunter, T. The protein kinase family: conserved features and deduced phylogeny of the catalytic domains. Science 1988, 241 (4861), 42-52.
4. Schultz, J.; Ferguson, B.; Sprague Jr, G. F. Signal transduction and growth control in yeast. Curr Opin Genet Dev 1995, 5 (1), 31-37.
5. Morgan, D. O. Principles of CDK regulation. Nature 1995, 374 (6518), 131-134.
6. Knighton, D. R.; Zheng, J.; Lynn, F. T. E.; Ashford, V. A.; Xuong, N.-H.; Taylor, S. S.; Sowadski, J. M. Crystal Structure of the Catalytic Subunit of Cyclic Adenosine Monophosphate-Dependent Protein Kinase. Science 1991, 253 (5018), 407-414.

7. Zhang, F.; Strand, A.; Robbins, D.; Cobb, M. H.; Goldsmith, E. J. Atomic structure of the MAP kinase ERK2 at 2.3 A resolution. Nature 1994, 367 (6465), 704-711.
8. Xu, R. M.; Carmel, G.; Sweet, R. M.; Kuret, J.; Cheng, X. Crystal structure of casein kinase-1, a phosphate-directed protein kinase. EMBO J 1995, 14 (5), 1015-1023.
9. Owen, D. J.; Noble, M. E. M.; Garman, E. F.; Papageorigiou, A. C.; Johnson, L. N. Two structures of the catalytic domain of phosphorylase kinase: an active protein kinase complexed with substrate analogue and product. Structure 1995, 3 (5), 467-482.
10. De Bondt, H. L.; Rosenblatt, J.; Jancarik, J.; Jones, H. D.; Morgant, D. O.; Kim, S.-H. Crystal structure of cyclin-dependent kinase 2. Nature 1993, 363 (6430), 595-602.
11. Taylor, S. S.; Radzio-Andzelm, E. Three protein kinase structures define a common motif. Structure 1994, 2 (5), 345-355.
12. Casimiro, M. C.; Crosariol, M.; Loro, E.; Li, Z.; Pestell, R. G. Cyclins and Cell Cycle Control in Cancer and Disease. Genes Cancers 2012, 3 (11-12), 649-657.
13. Otto, T.; Sicinski, P. Cell cycle proteins as promising targets in cancer therapy. Nat Rev Cancer 2017, 17 (2), 93-115.
14. Johnson, E. F.; Stewart, K. D.; Woods, K. W.; Giranda, V. L.; Luo, Y. Pharmacological and Functional Comparison of the Polo-like Kinase Family: Insight into Inhibitor and Substrate Specificity. Biochemistry 2007, 46 (33), 9551-9563.
15. Harrington, E. A.; Bebbington, D.; Moore, J.; Rasmussen, R. K.; Ajose-Adeogun, A. O.; Nakayama, T.; Graham, J. A.; Demur, C.; Hercend, T.; Diu-Hercend, A.; Su, M.; Golec, J. M. C.; Miller, K. M. VX-680, a potent and selective small-molecule inhibitor of the Aurora kinases, suppresses tumor growth in vivo. Nat Med 2004, 10 (3), 262-267.
16. Kitagawa, M.; Okabe, T.; Ogino, H.; Matsumoto, H.; Suzuki-Takahashi, I.; Kokubo, T.; Higashi, H.; Saitoh, S.; Taya, Y.; Yasuda, H. Butyrolactone I, a selective inhibitor of cdk2 and cdc2 kinase. Oncogene 1993, 8 (9), 2425-2432.
17. Hochegger, H.; Takeda, S.; Hunt, T. Cyclin-dependent kinases and cell-cycle transitions: does one fit all? Nat Rev Mol Cell Biol 2008, 9 (11), 910-916.
18. Ekholm, S. V.; Reed, S. I. Regulation of G1 cyclin-dependent kinases in the mammalian cell cycle. Curr Opin Cell Biol 2000, 12 (6), 676-684.
19. Hanks, S. K. Genomic analysis of the eukaryotic protein kinase superfamily: a perspective. Genome Biol 2003, 4 (5), 111.
20. Peyressatre, M.; Prével, C.; Pellerano, M.; Morris, C. M.; Borges, F.; Roleira, F.; Milhazes, N.; Santana, L.; Uriarte, E. Targeting Cyclin-Dependent Kinases in Human Cancers: From Small Molecules to Peptide Inhibitors

Simple Coumarins and Analogues in Medicinal Chemistry: Occurrence, Synthesis and Biological Activity. Cancers 2015, 7 (1), 887-916.

21. Borges, F.; Roleira, F.; Milhazes, N.; Santana, L.; Uriarte, E. Simple Coumarins and Analogues in Medicinal Chemistry: Occurrence, Synthesis and Biological Activity. Curr Med Chem 2005, 12 (8), 887-916.
22. Ojala, T. Biological screening of plant coumarins. Academic Dissertation, University of Helsinky, Helsinki, 2001.
23. Hoult, J. R. S.; Payá, M. Pharmacological and biochemical actions of simple coumarins: Natural products with therapeutic potential. Gen Pharmacol Vasc Syst 1996, 27 (4), 713-722.
24. Finn, G. J.; Kenealy, E.; Creaven, B. S.; Egan, D. A. In vitro cytotoxic potential and mechanism of action of selected coumarins, using human renal cell lines. Cancer Lett 2002, 183 (1), 61-68.
25. Grötz, K. A.; Wüstenberg, P.; Kohnen, R.; Al-Nawas, B.; Henneicke-von Zepelin, H. H.; Bockisch, A.; Kutzner, J.; Naser-Hijazi, B.; Belz, G. G.; Wagner, W. Prophylaxis of radiogenic sialadenitis and mucositis by coumarin/troxerutine in patients with head and neck cancer – a prospective,randomized, placebo-controlled, double-blind study. Br J Oral Maxillofac Surg 2001, 39 (1), 34-39.
26. Holbrook, A. M. P., J. A.; Labiris, R.; McDonald, H.; Douketis, J. D.; Crowther, M.; Wells, P. S. Systematic overview of warfarin and its drug and food interactions. Arch Intern Med 2005, 165 (10), 1095-1106.
27. Jiménez-Orozco, F. A.; López-González, J. S.; Nieto-Rodriguez, A.; Velasco-Velázquez, M. A.; Molina-Guarneros, J. A.; Mendoza-Patiño, N.; García-Mondragón, M. J.; Elizalde-Galvan, P.; León-Cedeño, F.; Mandoki, J. J. Decrease of cyclin D1 in the human lung adenocarcinoma cell line A-427 by 7-hydroxycoumarin. Lung Cancer 2001, 34 (2), 185-194.
28. Yun, E.-S.; Park, S.-S.; Shin, H.-C.; Choi, Y. H.; Kim, W.-J.; Moon, S.-K. p38 MAPK activation is required for esculetin-induced inhibition of vascular smooth muscle cells proliferation. Toxicol In Vitro 2011, 25 (7), 1335-1342.
29. Marshall, M. E.; Kervin, K.; Benefield, C.; Umerani, A.; Albainy-Jenei, S.; Zhao, Q.; Khazaeli, M. B. Growth-inhibitory effects of coumarin (1,2-benzopyrone) and 7-hydroxycoumarin on human malignant cell lines in vitro. J Cancer Res Clin Oncol 1994, 120 (1), S3-S10.
30. Kawaii, S.; Tomono, Y.; Ogawa, K.; Sugiura, M.; Yano, M.; Yoshizawa, Y. The antiproliferative effect of coumarins on several cancer cell lines. Anticancer Res 2001, 21 (2A), 917-923
31. Marshall, M.; Butler, K.; Fried, A. Phase I evaluation of coumarin (1, 2-benzopyrone) and cimetidine in patients with advanced malignancies. Mol Biother 1991, 3 (3), 170-178.
32. Sharma, A.; Chowdhury, R.; Dash, S.; Pallavi, B.; Shukla, P. Fast Microwave Assisted Synthesis of Pyranopyrazole Derivatives as New Anticancer Agents. Curr Microwave Chem 2016, 3 (1), 78-84.
33. Schneider, G. Prediction of drug-like properties. In Madame Curie Bioscience

Database [Internet], Landes Bioscience: Austin, Texas, 2000-2013.
34. Schuttelkopf, A. W.; van Aalten, D. M. F. PRODRG: a tool for high-throughput crystallography of protein-ligand complexes. Acta Crystalogr D 2004**,** 60 (8), 1355-1363.
35. Jena, L.; Waghmare, P.; Kashikar, S.; Kumar, S.; Harinath, B. C. Computational approach to understanding the mechanism of action of isoniazid, an anti-TB drug. Int J Mycobacteriol 2014**,** 3 (4), 276-282.
36. Davis, A. M.; Teague, S. J.; Schultz, J.; Ferguson, B.; Sprague Jr, G. F. Hydrogen Bonding, Hydrophobic Interactions, and Failure of the Rigid Receptor Hypothesis. Angew Chem Int Ed 1999**,** 38 (6), 736-749.